Effect of Fractional calculus on surface deformation due to movement of a nonplanar dip-slip fault

Piu Kundu

Received: date / Accepted: date

Abstract The social and economic importance of earthquake prediction has long been obvious. Hence, developing an effective earthquake prediction program became the most important objective of researchers in earthquake seismology. Indestructible earthquakes are typically modeled as a simple planar fault plane or a combination of multiple planar fault segments. The present paper investigates the deforming phenomena of a nonplanar (containing three planar parts) dip-slip fault lying in a viscoelastic half-space of a Standard linear solid medium. The expressions of displacement due to the fault movement and stress-strain accumulation or releases on the ground deformation are deduced by inducing appropriate boundary conditions in Laplace transformation, Green's function, and fractional calculus techniques. The efficacy of different affecting parameters viz. dip angle of the fault with horizontal, distance of the fault from the free surface, velocity of the fault movement, and fractional order are portrayed graphically. A comparative study has been done to understand the effect of fractional derivatives on displacement and stress-strain accumulation or release. These results may help to study the subsurface deformation and its effect on fault movement, causing earthquakes.

Keywords Nonplanar Fault · Dip-slip Fault Movement · Integral Transform · Fractional Calculus Method · Green's Function Technique

1 Introduction

Fault geometry is a key factor controlling fault mechanics. These faults may be infinite faults (whose length is considerable compared to their width e.g.

Piu Kundu (Corresponding Author)
Department of Mathematics, VIT-AP University Inavolu, Beside AP Secretariat, Amaravati AP, India

Alaska-Aleutian Megathrust fault) of finite faults (whose length is not so large compare to its width, e.g. Aedipsos-Kandili fault). Also the movement of a fault can be along the strike-line (called strike-slip fault, e.g. Anatolian fault) or can be parallel with the dip of the fault (called dip-slip fault, e.g. Aedipsos Kandili fault). A fault is called a surface-breaking fault if the rapture is visible on the ground along the fault (e.g., Lost River fault) and a fault is called a buried fault if the rapture does not produce a visible offset on the ground along the fault (e.g. Northridge fault). Large earthquakes are typically modelled using simple planar fault planes or a combination of multiple planar fault segments. In general, however, earthquakes occur on non-planar faults with significant geometric changes in both strike and dip directions. The Ventura Basin contains a complex network of nonplanar faults which is located in the Transverse Mountains of southern California and ([26]). A earthquake of 7.2 magnitude struck Nippes, Haiti on 14 August 2021 which is a rupture due to a nonplanar dipping fault ([16]).

To understand the earthquake process in seismically active regions, it is necessary to develop theoretical models of the slow seismic ground deformations observed in seismically active areas during aseismic periods. Several dynamic models have been developed to study various fault systems by many researchers. Singleton et al. (2021)[30] discussed the current status of faults and underground structures in the San Diego Bay Pull-Apart Basin, California. Depending on the variation in size and orientation, one of a kind faults can produce extraordinary forms of rock deformation[see Bouchez and Nicolas (2021)[2]]. A Green's function method was initiated in a semi-infinite elastic medium by Steketee (1958a)[31] and (1958b)[32]. The analytical expression of displacement due to movement of a vertical rectangular fault in a semi-infinite elastic medium has been observed by Chinnery (1961)[8]). Near to the Earth's crust, the change of stress accumulation or releases in the neighborhood of fault's edge demonstrated by Chinnery (1963[9], 1964[10]). Maruyama (1964)[19] explained various models of containing earthquake fluctuations. One infinite fault model in standard linear solid medium has been studied by Mondal et al. (2020)[21]. One nonplanar fault model in viscoelastic half-space has been presented by Sen et al. (2012)[28]. A nonplanar fault model with two interconnected parts lying in an elastic layer over viscoelastic half space has been studied by Sen and Karmakar (2013)[29]. A three-dimensional mechanical model has been illustrated by Marshall et al. (2008[18]) which is incorporating both nonplanar and rectangular planar faults.

Keeping this in view, we introduce a model of nonplanar dip-slip fault containing three planar parts situated in a viscoelastic half-space of standard linear solid medium which explain the representation of the lithosphere-asthenosplere system. But, till date, no attampts were made to investigate such phenomena on an nonplanar fault structure. The fault model has been considered as a buried, nonplanar, inclined. The movement across the fault has been taken as creeping, aseismic and dip-slip type. After occurrence of a destructible earthquake, we study the fault movement and also analysis the effect of the fault on ground by obtaining displacement and stress-strain accumula-

tion and/or releases due to fault movement. Moreover, the integral transform, Green's function technique and fractional calculus method are introduced to derive the expressions of displacement and stress-strain accumulation or release. The effect of different affecting parameters viz. inclinations of the fault with the free surface, velocity of the fault movement, depth of the fault from the free surface and fractional order derivative on displacement and stress-strain components is illustrated graphically.

2 Mathematical Model

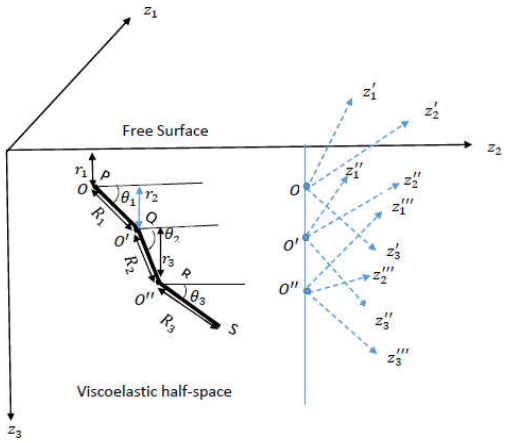

Fig. 1 *A simplified outlook of our model on the plane* $z_1 = 0$

To formulate the present problem, a theoretical model has been considered in lithosphere asthenosphere system as depicted through Fig. 1. The fault geometry is nonplanar and it contains three interconnected planar parts having different lengths and inclinations with horizontal. The nature of the fault is infinite, buried (at a finite depth from the free surface), inclined and the movement of the fault is dip-slip. The fault is situated in a viscoelastic half-space of Standard linear solid medium. A rectangular Cartesian coordinate system (z_1, z_2, z_3) is introduced with the free surface of the viscoelastic half-space. z_1 axis is extended parallel to the upper edge (strike) of the fault on free surface. z_3 axis is extended vertically downward into the half space and $z_3 \geq 0$. The fault contains three planar parts as $PQ = R_1$, $QR = R_2$ and $RS = R_3$ with corresponding inclination (with horizon) ϑ_1, ϑ_2 and ϑ_3 respectively. The total inclined depth across the fault is $R = R_1 + R_2 + R_3$. The depth of the planar parts PQ, QR, RS from the free surface are r_1, r_2, r_3 respectively. The fault parts PQ, QR, RS starts to move at time $t = T_1, T_2, T_3$ respectively. Since

the fault is buried and inclined then another three rectangular cartesian co-ordinate system (z_1', z_2', z_3'), (z_1'', z_2'', z_3'') and (z_1''', z_2''', z_3''') has been considered across the planar parts PQ, QR, RS, respectively. So the relation between (z_1, z_2, z_3) with (z_1', z_2', z_3'), (z_1'', z_2'', z_3'') and (z_1''', z_2''', z_3''') are respectively

$$\begin{aligned} z_1 &= z_1' \\ z_2 &= z_2' \sin\vartheta_1 + z_3' \cos\vartheta_1 \\ z_3 &= -z_2' \cos\vartheta_1 + z_3' \sin\vartheta_1 + r_1 \end{aligned} \tag{1}$$

$$\begin{aligned} z_1 &= z_1'' \\ z_2 &= z_2'' \sin\vartheta_2 + z_3'' \cos\vartheta_2 \\ z_3 &= -z^{2''} \cos\vartheta_2 + z^{3''} \sin\vartheta_2 + r_1 + r_2 \end{aligned} \tag{2}$$

and

$$\begin{aligned} z_1 &= z_1''' \\ z_2 &= z_2''' \sin\vartheta_3 + z_3''' \cos\vartheta_3 \\ z_3 &= -z^{2'''} \cos\vartheta_3 + z^{3'''} \sin\vartheta_3 + r_1 + r_2 + r_3 \end{aligned} \tag{3}$$

Let the displacement components along coordinate axes z_1, z_2, z_3 are v_1, v_2, v_3 respectively; γ_{11}, γ_{12}, γ_{13}, γ_{22}, γ_{23}, γ_{33} are the stress components and E_{11}, E_{12}, E_{13}, E_{22}, E_{23}, E_{33} are the strain components. Since the fault is taken to be very long along z_1 axis compare to its depth, so all the displacement, stress-strain components independent on z_1 axis and become function of z_2, z_3 and time t. The displacement, stress and strain components categorize into two groups - one group corresponding with strike-slip movement (v_1; γ_{12}, γ_{13}; E_{12}, E_{13}) and other ground corresponding with dip-slip movement(v_2, v_3; γ_{22}, γ_{23}, γ_{33}; E_{22}, E_{23}, E_{33}) (Mukhopadhyay et al. 1980a[**?**], 1980b[24]). In the present study, we consider the second group only. The preliminary observation commences in a scenario when the fault movement does not present in the medium that is the time at $t = 0$ and the viscoelastic medium is in a quasi static aseismic state but a very slow aseismic deformation occurs continuously. These movement are sustained by various tectonic forces including mantel convection, internal pressure within the earth and other geological changes. The components of displacement, stress and strain satisfy certain constitutive equations, stress-equation of motion and boundary conditions for an instant $t \geq 0$ whrich are illustrated below.

2.1 Constitutive Equation

The constitutive equations for dip-slip fault in a visco-elastic half-space of fractional order Standard linear solid medium (Segall[27]) at time t are

$$\begin{aligned} \gamma_{22} + \frac{\eta}{\mu}\frac{\partial^\alpha}{\partial t^\alpha}(\gamma_{22}) &= \mu\frac{\partial v_2}{\partial z_2} + 2\eta\frac{\partial^\alpha}{\partial t^\alpha}\frac{\partial v_2}{\partial z_2} \\ \gamma_{23} + \frac{\eta}{\mu}\frac{\partial^\alpha}{\partial t^\alpha}(\gamma_{23}) &= \frac{\mu}{2}\left(\frac{\partial v_2}{\partial z_3} + \frac{\partial v_3}{\partial z_2}\right) + \eta\frac{\partial^\alpha}{\partial t^\alpha}\left(\frac{\partial v_2}{\partial z_3} + \frac{\partial v_3}{\partial z_2}\right) \\ \gamma_{33} + \frac{\eta}{\mu}\frac{\partial^\alpha}{\partial t^\alpha}(\gamma_{33}) &= \mu\frac{\partial v_3}{\partial z_3} + 2\eta\frac{\partial^\alpha}{\partial t^\alpha}\frac{\partial v_3}{\partial z_3} \end{aligned} \qquad (4)$$

where $\frac{\partial^\alpha}{\partial t^\alpha}$ is the fractional operator of order α ($0 < \alpha \leq 1$), η appears for viscosity of the material and μ represents rigidity of the material.

In this study, we are considering the Caputo fractional derivative (Caputo[6], 1969), which is defined by

$$\frac{\partial^\alpha}{\partial t^\alpha} f(t) = \frac{1}{\Gamma(n-\alpha)} \int_0^t \frac{\frac{\partial^n}{\partial t^n} f(\xi)}{(t-\xi)^{\alpha-n+1}} d\xi$$

where $n-1 < \alpha < n$ such that n is defined by

$$n = \begin{cases} [\alpha] + 1 \text{ if } \alpha \notin N \cup 0 \\ \alpha + 1 \text{ if } \alpha \in N \cup 0 \end{cases}$$

2.2 Stress Equation of Motion

We start our observation when there is no seismic activity present in the medium and that time is taken to be $t = 0$. The gradual aseismic, quasi-static deformation implies that inertial forces are negligible (Mukhopadhyay et al. 1980a[24]). Additionally, considering the initial stress level as the reference point, there is no alteration in body forces across the medium. So, the relative change in body forces can be considered as zero. Hence, the stress equation of motion for dip-slip fault can be written as

$$\begin{aligned} \frac{\partial}{\partial z_2}(\gamma_{22}) + \frac{\partial}{\partial z_3}(\gamma_{23}) &= 0 \\ \frac{\partial}{\partial z_2}(\gamma_{32}) + \frac{\partial}{\partial z_3}(\gamma_{33}) &= 0 \end{aligned} \qquad (5)$$

2.3 Boundary condition

The boundary conditions for $|z_2| \to \infty$, $z_3 \geq 0$ is

$$\gamma_{22}(z_2, z_3, t) = \gamma_\infty(0)(1 + kt)\cos\vartheta_1 \qquad (6)$$

where $\gamma_\infty(t)$ represents tectonic deformation that acts far from the fault due to mantle convection in the lithospheric-asthenospheric system and causes slip

motion across the fault. $\gamma_\infty(t)$ is obtain as $\gamma_\infty(0)(1 + kt)$, where $k > 0$ so that the tectonic forces increases linearly with time.

At $z_3 = 0$

$$\begin{matrix} \gamma_{23} = 0 \\ \gamma_{33} = 0 \end{matrix} \tag{7}$$

where $-\infty < z_2 < \infty$ and $t \geq 0$.

Also as $z_3 \to \infty$ and for $-\infty < z_2 < \infty,\ t \geq 0$,

$$\begin{matrix} \gamma_{23}(z_2, z_3, t) \to 0 \\ \gamma_{33}(z_2, z_3, t) \to \gamma_\infty(0)(1 + kt) \sin \vartheta_1 \end{matrix} \tag{8}$$

where $\gamma_\infty(0) = \gamma_\infty(t)|_{t=0}$.

2.4 Initial Condition

The initial values of displacement, stress and strain components are taken as $(v_i)_0$, $(\gamma_{ij})_0$ and $(E_{ij})_0$.

3 Solution

Equation (4) may be written as

$$\begin{matrix} \gamma_{22} + \frac{\eta}{\mu}\frac{\partial^\alpha}{\partial t^\alpha}(\gamma_{22}) = \mu\frac{\partial v_2}{\partial z_2} + 2\eta\frac{\partial^\alpha}{\partial t^\alpha}\frac{\partial v_2}{\partial z_2} \\ \gamma_{23} + \frac{\eta}{\mu}\frac{\partial^\alpha}{\partial t^\alpha}(\gamma_{23}) = \mu\frac{\partial v_2}{\partial z_3} + 2\eta\frac{\partial^\alpha}{\partial t^\alpha}\frac{\partial v_2}{\partial z_3} \\ \gamma_{23} + \frac{\eta}{\mu}\frac{\partial^\alpha}{\partial t^\alpha}(\gamma_{23}) = \mu\frac{\partial v_3}{\partial z_2} + 2\eta\frac{\partial^\alpha}{\partial t^\alpha}\frac{\partial v_3}{\partial z_2} \\ \gamma_{33} + \frac{\eta}{\mu}\frac{\partial^\alpha}{\partial t^\alpha}(\gamma_{33}) = \mu\frac{\partial v_3}{\partial z_3} + 2\eta\frac{\partial^\alpha}{\partial t^\alpha}\frac{\partial v_3}{\partial z_3} \end{matrix} \tag{9}$$

Applying differentiation method on first and second equation of (9) w.r.t z_2 and z_3 respectively, then adding and with aid of equation of (5) it is found that, $\frac{\partial^\alpha}{\partial t^\alpha}\nabla^2 v_2 = -\frac{\mu}{2\eta}\nabla^2 v_2$ and $\frac{\partial^\alpha}{\partial t^\alpha}\nabla^2 v_3 = -\frac{\mu}{2\eta}\nabla^2 v_3$

neglecting 1st and higher order derivative of v_1, v_2 and using initial condition $v_2|_{t=0} = (v_2)_0$ and $v_3|_{t=0} = (v_3)_0$ on the above expression we get

$$\nabla^2 V_2 = 0, \text{ where } V_2 = v_2 - (v_2)_0 E_\alpha\left(-\frac{\mu}{2\eta}t^\alpha\right) \tag{10}$$

and

$$\nabla^2 V_3 = 0, \text{ where } V_3 = v_3 - (v_3)_0 E_\alpha\left(-\frac{\mu}{2\eta}t^\alpha\right) \tag{11}$$

where $E_\alpha(-\frac{\mu}{2\eta}t^\alpha)$ is Mittage-Leffler function.

The final solutions for displacement, stress and strain transform to

$$\begin{aligned} v_i &= \sum_{k=1}^{4} (v_i)_k \ (i = 2, 3) \\ \gamma_{ij} &= \sum_{k=1}^{4} (\gamma_{ij})_k, \ (i, j = 2, 3) \\ E_{ij} &= \sum_{k=1}^{4} (e_{ij})_k, \ (i, j = 2, 3) \end{aligned} \tag{12}$$

where $(v_i)_1$ $(i = 2, 3)$, $(\gamma_{ij})_1$ and $(E_{ij})_1$ $(i, j = 2, 3)$ are components of displacement, stress and strain respectively in the absence of fault movement; $(v_i)_2$ $(i = 2, 3)$, $(\gamma_{ij})_2$, $(E_{ij})_2$ $(i, j = 2, 3)$ are components displacement, stress and strain respectively due to movement of planar part PQ; $(v_i)_3$ $(i = 2, 3)$, $(\gamma_{ij})_3$, $(E_{ij})_3$ $(i, j = 2, 3)$ are components displacement, stress and strain respectively due to movement of planar part QR; $(v_i)_4$ $(i = 2, 3)$, $(\gamma_{ij})_4$, $(E_{ij})_4$ $(i, j = 2, 3)$ are components displacement, stress and strain respectively across the planar part RS.

3.1 Derivation of the components of displacement and stress-strain in the absence of fault movement

Now for solving the above boundary value problem, Laplace transform has been taken on all the stress equation of motion (5), boundary conditions (6 to 8)and governing equations (10 & 11) respectively, we obtain

$$\begin{aligned} \frac{\partial}{\partial z_2}(\bar{\gamma}_{22}) + \frac{\partial}{\partial z_3}(\bar{\gamma}_{23}) &= 0 \\ \frac{\partial}{\partial z_2}(\bar{\gamma}_{32}) + \frac{\partial}{\partial z_3}(\bar{\gamma}_{33}) &= 0 \end{aligned} \tag{13}$$

$$\bar{\gamma}_{22} = \gamma_\infty(0)\left(\frac{1}{s} + \frac{k}{s^2}\right)\cos\vartheta_1 \text{ for } z_3 \geq 0 \tag{14}$$

$$\begin{aligned} &\bar{\gamma}_{23} = \bar{\gamma}_{33} = 0 \text{ for } z_3 = 0 \\ &\bar{\gamma}_{23}(z_2, z_3, t) \to 0 \ \text{ for } z_3 \to 0 \\ &\bar{\gamma}_{33} \to \gamma_\infty(0)\left(\frac{1}{s} + \frac{k}{s^2}\right)\sin\vartheta_1 \ \text{ for } z_3 \to 0 \end{aligned} \tag{15}$$

$$\begin{aligned} &\nabla^2 \bar{V}_2 = 0, \ \text{where} \ \bar{v}_2 = (v_2)_0 \frac{s^{\alpha-1}}{s^\alpha + \frac{\mu}{2\eta}} \\ &\nabla^2 \bar{V}_3 = 0, \ \text{where} \ \bar{v}_3 = (v_3)_0 \frac{s^{\alpha-1}}{s^\alpha + \frac{\mu}{2\eta}} \end{aligned} \tag{16}$$

Let us assume the trial solution of (16) by assuming initial displacement field as zero:

$$\bar{v}_2 = \frac{s^{\alpha-1}}{s^\alpha + \frac{\mu}{2\eta}}(v_2)_0 + a_1 z_2 + b_1 z_3 \tag{17}$$

$$\bar{v}_3 = \frac{s^{\alpha-1}}{s^\alpha + \frac{\mu}{2\eta}}(v_3)_0 + a_2 z_2 + b_2 z_3 \tag{18}$$

where a_1, b_1, a_2, b_2 are constant or function of z_2 and z_3.

Now taking Laplace transform on constitutive equation (5), neglecting first and higher order derivative of v_2 and v_3 and using the value of $\bar{v}_2$ and $\bar{v}_3$ we obtain,

$$\begin{aligned}
&(1+\tfrac{\eta}{\mu}s^{\alpha})\bar{\gamma}_{22} - \tfrac{\eta}{\mu}s^{\alpha-1}(\gamma_{22})_0 = a_1(\mu+2\eta s^{\alpha}) \\
&(1+\tfrac{\eta}{\mu}s^{\alpha})\bar{\gamma}_{23} - \tfrac{\eta}{\mu}s^{\alpha-1}(\gamma_{23})_0 = \tfrac{1}{2}(a_2+b_1)(\mu+2\eta s^{\alpha}) \\
&(1+\tfrac{\eta}{\mu}s^{\alpha})\bar{\gamma}_{33} - \tfrac{\eta}{\mu}s^{\alpha-1}(\gamma_{33})_0 = b_2(\mu+2\eta s^{\alpha})
\end{aligned} \tag{19}$$

Using Eqs. (14 & 15) in Eq. (19) we have,

$$\begin{aligned}
(v_2)_1 &= (v_2)_0 E_{\alpha}(-\tfrac{\mu}{2\eta}t^{\alpha}) + \tfrac{\gamma_{\infty}(0)\cos\vartheta_1}{\mu}z_2\left[(1-\tfrac{\eta k}{\mu})(1-E_{\alpha}(-\tfrac{\mu}{2\eta}t^{\alpha})) + kt\right] \\
(v_3)_1 &= (v_3)_0 E_{\alpha}(-\tfrac{\mu}{2\eta}t^{\alpha}) + \tfrac{\gamma_{\infty}(0)\sin\vartheta_1}{\mu}z_3\left[(1-\tfrac{\eta k}{\mu})(1-E_{\alpha}(-\tfrac{\mu}{2\eta}t^{\alpha})) + kt\right] \\
(\gamma_{22})_1 &= (\gamma_{22})_0 E_{\alpha}(-\tfrac{\mu}{\eta}t^{\alpha}) + \gamma_{\infty}(0)\cos\vartheta_1(1+kt-E_{\alpha}(-\tfrac{\mu}{2\eta}t^{\alpha})) \\
(\gamma_{23})_1 &= (\gamma_{23})_0 E_{\alpha}(-\tfrac{\mu}{2\eta}t^{\alpha}) \\
(\gamma_{33})_1 &= (\gamma_{33})_0 E_{\alpha}(-\tfrac{\mu}{\eta}t^{\alpha}) + \gamma_{\infty}(0)\sin\vartheta_1(1+kt-E_{\alpha}(-\tfrac{\mu}{2\eta}t^{\alpha})) \\
(E_{22})_1 &= (E_{22})_0 E_{\alpha}(-\tfrac{\mu}{2\eta}t^{\alpha}) + \tfrac{\gamma_{\infty}(0)\cos\vartheta_1}{\mu}\left[(1-\tfrac{\eta k}{\mu})(1-E_{\alpha}(-\tfrac{\mu}{2\eta}t^{\alpha})) + kt\right] \\
(E_{23})_1 &= (E_{23})_0 E_{\alpha}(-\tfrac{\mu}{2\eta}t^{\alpha}) \\
(E_{33})_1 &= (E_{33})_0 E_{\alpha}(-\tfrac{\mu}{2\eta}t^{\alpha}) + \tfrac{\gamma_{\infty}(0)\sin\vartheta_1}{\mu}\left[(1-\tfrac{\eta k}{\mu})(1-E_{\alpha}(-\tfrac{\mu}{2\eta}t^{\alpha})) + kt\right]
\end{aligned} \tag{20}$$

From the expression of γ_{22} and γ_{33} in (20) it is obtained that the resultant stress parallel to the fault plane with y_2 and y_3 directions is an expanding function of t and depends on both horizontal and vertical directions. At t = 0, the stresses attend initial stress values $(\gamma_{22})_0$ and $(\gamma_{33})_0$ and after that it is increasing gradually with respect to time and ultimately converges $\gamma_{\infty}(0)\cos\vartheta_1(1+kt)$ and $\gamma_{\infty}(0)\sin\vartheta_1(1+kt)$ respectively. The rheological behavior of viscoelastic material near to the fault plane state that there are some threshold amount of stress in the material (say γ_c) called the critical value of stress and also it is taken that $|\gamma_c|$ <[Stress value on right hand side boundary]. Therefore, after a certain time T_1 (critical time level), when in the neighbourhood of fault the accumulated stress overcome the critical stress level , a fault movement take place across the fault plane.In this model, it is obtain that the fault begins to slip when the resulting stress exceeds a critical value (γ_c) at the critical time T_1 .

3.2 Derivation of displacement and stress-strain field after the fault movement

Now we obtain a solution of our problem in view of that across the fault plane, the movement across the fault has been occurred due to overcome of the critical stress level by the average stress over the fault at T_1 . In view of (1) to (8 with an extra condition of discontinuity in displacement components v_3 due to dislocation across the fault as follows:

$$[v_3]_{PQ} = W_1(t_1)\, f(z'_3)\, H(t_1) \qquad (z'_2 = 0,\ 0 \le z'_3 \le R_1,\ t_1 \ge 0,\ t_1 = t - T_1) \tag{21}$$

where $[v_3]$ denotes the relative displacement having a discontinuity which is described as

$$[v_3]_{PQ} = \lim_{(z'_2 \to 0^+)} (v_3) - \lim_{(z'_2 \to 0^-)} (v_3) \tag{22}$$

$W_1(t_1) = w_1 t_1$ represents the dislocation at the upper edge of PQ part, w_1 is the velocity of movement of PQ, $H(t_1)$ is the Heaviside step function whose value is obtained as 1 for $t_1 > 0$ and $f(z'_3)$ is the depth dependent dislocation function where variable z'_3 varies from the free surface to downward direction over the fault crack on $z_1 = 0$. The value of the heaviside function

Then equation (21) is articulated as

$$[v_3]_{PQ} = W_1(t_1) f(z'_3) \tag{23}$$

Taking Laplace transform on equation (23)

$[\bar{v}_3]_{PQ} = W_1(s)\, f(z'_3)$, where $\bar{v}_3$ is the Laplace transform of v_3 and 's' is the Laplace transform variable with respect to time.

For $t_1 \le 0$, $[(v_3)]_{PQ} = 0$.

The solutions of displacement, stress and strain components after the creeping movement across the planar part PQ are obtained by using Greens function technique and Laplace transform. A suitable modified form of Greens function technique developed by Maruyamma (1964 [19], 1966[20]) and Rybicki (1971 [25]). Following Maruyamma (1966)

$$(\bar{v}_3)_2(Q_1) = \int_{PQ} [(\bar{v}_3)_2(s)]\, [G'_{33}(Q_1, P_1)\, d\xi_2 - G_{32}(Q_1, P_1)\, d\xi_3] \tag{24}$$

where $Q_1(z_1, z_2, z_3)$ represents field point in half-space, $P_1(\xi_1, \xi_2, \xi_3)$ is any point on the fault PQ. $0 \le \xi_2 \le l_1 \cos\vartheta_1$, $0 \le \xi_3 \le l_1 \sin\vartheta_1$, and $\xi_2 = \xi_3 \cot\vartheta_1$.

Since the inclined angle across PQ is ϑ_1 with the free surface than the transformation of co-ordinate system (ξ_1, ξ_2, ξ_3) to (ξ'_1, ξ'_2, ξ'_3) is illustrated as

$$\begin{aligned} \xi_1 &= \xi_1' \\ \xi_2 &= \xi_2' \sin\vartheta_1 + \xi_3' \cos\vartheta_1 \\ \xi_3 &= -\xi_2' \cos\vartheta_1 + \xi_3' \sin\vartheta_1 + r_1 \end{aligned} \quad \vdots \quad (25)$$

From $\xi_2 = \xi_3 \cot\vartheta_1$ it is found that, $\xi_2' = 0$

Then from equation (25), $\xi_1 = \xi_1'$, $\xi_2 = \xi_3' \cos\vartheta_1$ and $\xi_3 = \xi_3' \sin\vartheta_1 + r_1$

So, $d\xi_1 = d\xi_1'$, $d\xi_2 = \cos\vartheta_1 d\xi_2'$ and $d\xi_3 = \sin\vartheta_1 d\xi_3'$

Now it is assumed that $G_{33}' = \frac{1}{2\pi}[\frac{z_3-\xi_3}{L^2} - \frac{z_3+\xi_3}{M^2}]$ and $G_{32}' = \frac{1}{2\pi}[\frac{z_2-\xi_2}{L^2} + \frac{z_2-\xi_2}{M^2}]$ where $L^2 = (z_2 - \xi_2)^2 + (z_3 - \xi_3)^2$ and $M^2 = (z_2 - \xi_2)^2 + (z_3 + \xi_3)^2$

$(\bar{v}_3)_2 (Q_1) = \frac{W_1(s)}{2\pi}\psi^1(z_2, z_3)$

Taking inverse Laplace transform, $(v_3)_2 = \frac{W_1(t_1)}{2\pi}H(t - T_1)\psi^1(z_2, z_3)$ where

$$\psi^1 = \int_0^{R_1} f(\xi_3')[\frac{(z_2\sin\vartheta_1 - z_3\cos\vartheta_1) + r_1\cos\vartheta_1}{\xi_3'^2 - 2\xi_3'(z_2\cos\vartheta_1 + z_3\sin\vartheta_1) + (z_2^2 + z_3^2) + r_1^2 - 2z_3r_1 - 2r_1\xi_3'\sin\vartheta_1} + \frac{(z_2\sin\vartheta_1 + z_3\cos\vartheta_1) + r_1\cos\vartheta_1}{\xi_3'^2 - 2\xi_3'(z_2\cos\vartheta_1 - z_3\sin\vartheta_1) + (z_2^2 + z_3^2) + r_1^2 + 2z_3r_1 + 2r_1\xi_3'\sin\vartheta_1}]d\xi_3'$$

It is to be illustrated that for $t_1 = t - T_1 \leq 0$, $v_3 = 0$.

Since after the fault slip v_2 is continuous then due to the movement across PQ for $t_1 \geq 0$, $v_2 = 0$.

Then $(\bar{\gamma}_{22})_2 = 0$

Taking inverse Laplace transform $(\gamma_{22})_2 = 0$.

Now $(\bar{\gamma}_{23})_2 = \frac{s^\alpha}{\frac{1}{\eta} + \frac{s^\alpha}{\mu}}\frac{\partial \bar{v}_3}{\partial z_2} = \frac{s^\alpha}{\frac{1}{\eta} + \frac{s^\alpha}{\mu}}\frac{W_1(s)}{2\pi}\psi_2^1$, where $\psi_2^1 = \frac{\partial \psi^1}{\partial z_2}$

Taking inverse Laplace transform w.r.t t_1 and noting that $(\bar{\gamma}_{23})_2 = 0$ for $t_1 \leq 0$

$(\gamma_{23})_2 = \frac{\mu}{2}\frac{W_1(t_1)}{2\pi}\psi_2^1 H(t_1)[t_1 + \frac{\eta}{\mu}(1 - E_\alpha(-\frac{\mu}{\eta}t_1^\alpha))]$

Similarly $(\gamma_{33})_2 = \frac{\mu}{2}\frac{W_1(t_1)}{2\pi}\psi_3^1 H(t_1)[t_1 + \frac{\eta}{\mu}(1 - E_\alpha(-\frac{\mu}{\eta}t_1^\alpha))]$

Also $(E_{23})_2 = H(t_1)\frac{V_1(t_1)}{4\pi}\psi_2^1$

and

$(E_{33})_2 = H(t_1)\frac{V_1(t_1)}{4\pi}\psi_3^1$

The solutions of displacement, stress and strain components after the movement of PQ part are as follows:

$$\begin{aligned}
(v_3)_2 &= \tfrac{w_1(t_1)}{2\pi} H(t - T_1)\psi^1(z_2,\ z_3) \\
(\gamma_{22})_2 &= 0 \\
(\gamma_{23})_2 &= \tfrac{\mu\, w_1}{2\ 2\pi}\psi^1_2 H(t_1)[t_1 + \tfrac{\eta}{\mu}(1 - E_\alpha(-\tfrac{\mu}{\eta}t_1^\alpha))] \\
(\gamma_{33})_2 &= \tfrac{\mu\, w_1}{2\ 2\pi}\psi^1_3 H(t_1)[t_1 + \tfrac{\eta}{\mu}(1 - E_\alpha(-\tfrac{\mu}{\eta}t_1^\alpha))] \\
(E_{22})_2 &= 0 \\
(E_{23})_2 &= \tfrac{w_1 t_1}{2\pi} H(t_1)\psi^1_2(z_2,\ z_3) \\
(E_{33})_2 &= \tfrac{w_1 t_1}{2\pi} H(t_1)\psi^1_3(z_2,\ z_3)
\end{aligned} \qquad (26)$$

where $\psi^1_2 = \frac{\partial \psi^1}{\partial z_2}$ and $\psi^1_3 = \frac{\partial \psi^1}{\partial z_3}$

The shifting of origin also helps us to obtain the displacement, stress-strain components for second planar part QR as follows

$$\begin{aligned}
(v_3)_3 &= \tfrac{w_2(t_2)}{2\pi} H(t - T_2)\psi^2(z_2,\ z_3) \\
(\gamma_{22})_3 &= 0 \\
(\gamma_{23})_3 &= \tfrac{\mu\, w_2}{2\ 2\pi}\psi^2_2 H(t_2)[t_2 + \tfrac{\eta}{\mu}(1 - E_\alpha(-\tfrac{\mu}{\eta}t_2^\alpha))] \\
(\gamma_{33})_3 &= \tfrac{\mu\, w_2}{2\ 2\pi}\psi^2_3 H(t_2)[t_2 + \tfrac{\eta}{\mu}(1 - E_\alpha(-\tfrac{\mu}{\eta}t_2^\alpha))] \\
(E_{22})_3 &= 0 \\
(E_{23})_3 &= \tfrac{w_2 t_2}{2\pi} H(t_2)\psi^2_2(z_2,\ z_3) \\
(E_{33})_3 &= \tfrac{w_2 t_2}{2\pi} H(t_2)\psi^2_3(z_2,\ z_3)
\end{aligned} \qquad (27)$$

where where $\psi^2_2 = \frac{\partial \psi^2}{\partial z_2}$, $\psi^2_3 = \frac{\partial \psi^2}{\partial z_3}$ and the discontinuity in v_3 due to dislocation across QR results in:

$$[v_3]_{QR} = W_2(t_2)\, f(z_3'')\, H(t_2) \qquad (z_2'' = 0,\ 0 \le z_3'' \le R_2,\ t_2 \ge 0,\ t_2 = t - T_2) \qquad (28)$$

where $[v_3]$ denotes the relative displacement across QR, $W_2(t_2) = w_2 t_2$, w_2 is the velocity of movement of QR, $H(t_2)$ is the Heaviside step function and $f(z_3'')$ is the dislocation function depends on depth.

$$[v_3]_{QR} = \lim_{(z_2'' \to 0^+)} (v_3) - \lim_{(z_2'' \to 0^-)} (v_3) \qquad (29)$$

and

$$\psi^2 = \int_{R_1}^{R_2} f(\xi_3'')\Big[\frac{((z_2)\sin\vartheta_2 - z_3\cos\vartheta_2) + (r_1+r_2)\cos\vartheta_2}{\xi_3''^2 - 2\xi_3''((z_2)\cos\vartheta_2 + z_3\sin\vartheta_2) + ((z_2)^2 + z_3^2) + (r_1+r_2)^2 - 2z_3(r_1+r_2) - 2(r_1+r_2)\xi_3''\sin\vartheta_2} +$$

$$\frac{((z_2)\sin\vartheta_2 + z_3\cos\vartheta_2) + (r_1+r_2)\cos\vartheta_2}{\xi_3''^2 - 2\xi_3''((z_2)\cos\vartheta_2 - z_3\sin\vartheta_2) + ((z_2)^2 + z_3^2) + (r_1+r_2)^2 + 2z_3(r_1+r_2) + 2(r_1+r_2)\xi_3''\sin\vartheta_2}\Big] d\xi''$$

Similarly, for the other branch RS, we obtain respective solutions of displacement, stress-strain components as follows

$$\begin{aligned}
(v_3)_4 &= \frac{w_3(t_3)}{2\pi} H(t - T_3)\psi^3(z_2,\ z_3) \\
(\gamma_{22})_4 &= 0 \\
(\gamma_{23})_4 &= \frac{\mu\, w_3}{2\ 2\pi}\psi^3_2 H(t_3)[t_3 + \frac{\eta}{\mu}(1 - E_\alpha(-\frac{\mu}{\eta}t_3^\alpha))] \\
(\gamma_{33})_4 &= \frac{\mu\, w_3}{2\ 2\pi}\psi^3_3 H(t_3)[t_3 + \frac{\eta}{\mu}(1 - E_\alpha(-\frac{\mu}{\eta}t_3^\alpha))] \\
(E_{22})_4 &= 0 \\
(E_{23})_4 &= \frac{w_3 t_3}{2\pi} H(t_3)\psi^3_2(z_2,\ z_3) \\
(E_{33})_4 &= \frac{w_3 t_3}{2\pi} H(t_3)\psi^3_3(z_2,\ z_3)
\end{aligned} \tag{30}$$

where $\psi^3_2 = \frac{\partial \psi^3}{\partial z_2}$, $\psi^3_3 = \frac{\partial \psi^3}{\partial z_3}$ and also the discontinuity in displacement across RS as follows:

$$[v_3]_{RS} = W_3(t_3)\, f(z'''_3)\, H(t_3) \qquad (z'''_2 = 0,\ 0 \le z'''_3 \le R_3,\ t_3 \ge 0,\ t_3 = t - T_3) \tag{31}$$

where $W_3(t_3) = w_3 t_3$ proposed the dislocation across RS part, w_3 is the velocity of movement of RS, $H(t_2)$ is the Heaviside step function and $f(z''_3)$ is the dislocation function depends on depth.

$$[v_3]_{RS} = \lim_{(z'''_2 \to 0^+)} (v_3) - \lim_{(z'''_2 \to 0^-)} (v_3) \tag{32}$$

and

$$\psi^3 = \int_{R_2}^{R_3} f(\xi'''_3)\Big[\frac{((z_2)\sin\vartheta_3 - z_3\cos\vartheta_3) + (r_1+r_2+r_3)\cos\vartheta_3}{\xi'''^2_3 - 2\xi'''_3((z_2)\cos\vartheta_3 + z_3\sin\vartheta_3) + ((z_2)^2 + z_3^2) + (r_1+r_2+r_3)^2 - 2z_3(r_1+r_2+r_3) - 2(r_1+r_2+r_3)\xi'''_3\sin\vartheta_3} + \frac{((z_2)\sin\vartheta_3 + z_3\cos\vartheta_3) + (r_1+r_2+r_3)\cos\vartheta_3}{\xi'''^2_3 - 2\xi'''_3((z_2)\cos\vartheta_3 - z_3\sin\vartheta_3) + ((z_2)^2 + z_3^2) + (r_1+r_2+r_3)^2 + 2z_3(r_1+r_2+r_3) + 2(r_1+r_2+r_3)\xi'''_3\sin\vartheta_3}\Big] d\xi'''$$

4 Numerical Computations

We have analyzed the displacements, stresses and strains components succeeding the restoration of fault movement for different inclinations, different creep velocities and different orders of the fractional derivative by introducing suitable parametric values of the model parameters from Sen and Karmakar (2013)[29], Sen et al. (2012)[28], Mondal et al. (2019)[22], Debnath and Sen (2014[4], 2015[5]), which are relevant to the real world fault system. It is studied that the depth of the fault consider in between 10 to 15 km and therefore we assume as R_1 = 5.5 km, R_2 = 5 km and R_3 = 4.5 km that is, total arc length is R = 15 km. The inclined angle with horizontals are taken as $\vartheta_1,\ \vartheta_2,\ \vartheta_3 = \frac{\pi}{6}, \frac{\pi}{4}, \frac{\pi}{3}, \frac{\pi}{2}$

From various geological models on Lithosphere-asthenosphere system of the articles Cathles (1975) [3], Aki and Richard (2002)[1], Fowler (1983)[13],

Chift et al. (2002)[7], Karato (2020)[14] and from the recent studies Kundu et al. (2021)[15], the value of rigidity (μ) and viscosity (η) are taken as follows: $\mu = 3.5 \times 10^{10}\ N/m^2$, $\eta = 3 \times 10^{20}\ N/m^2$,

Depth of the planar parts r_1, r_2 and r_3 are taken as 5 km, 10 km and 15 km respectively.

The creep velocity across the planar parts due to fault movement is taken as $w_1, w_2, w_3 = 0.01, 0.02, 0.03, 0.04$ meter/year.

Since fractional order $\alpha \in (0, 1]$, we consider $\alpha = 0.1, 0.4, 0.7, 1$ for the observation.

The initial values of γ_{22}, γ_{23} and γ_{33} are taken as $(\gamma_{22})_0$, $(\gamma_{23})_0$ and $(\gamma_{33})_0 = 30 \times 10^5\ N/m^2$. Initial stress at infinity $(\gamma_\infty(0)) = 30 \times 10^5\ N/m^2$.

The critical stress level has been considered as $\gamma_c = 200$ bar (from Debnath and Sen (2014) [4]). So, in equation (20), γ_{22} and γ_{33} overreach this critical stress level after 111.08 years approximately. So, for our calculation, the critical time (T_1) has been observed as 111.08 years .

Creep functions are taken as from (Mondal and Debsarma [23])

$$f(z_3') = \frac{1}{2}\left[1 - 2\left(\frac{z_3'}{R_1'}\right)^2 + \left(\frac{z_3'}{R_1'}\right)^4\right]^{\frac{1}{2}} \text{ across PQ}$$

$$f(z_3'') = \frac{1}{6}\left[3 - \left(\sqrt{3} - \sqrt{-2}\right)\left(\frac{z_3'' - R_1}{R_2}\right)\right] \text{ across QR and}$$

$$f(z_3''') = \frac{1}{6}\left[1 - 6^5\left(\frac{z_3''' - R_1 - R_2}{R_3}\right)^2 + 3\left(\frac{z_3''' - R_1 - R_2}{R_3}\right)^3\right]^{\frac{1}{2}} \text{ across RS}$$

5 Result and Discussion

5.1 Effect of inclination of the fault:

Fig. 2 (a) and (b) represent the variation of rate of displacement (v_3) in vertically downwards direction due to movement of non-planar dip-slip fault for several values of inclination (ϑ_1) across the planar part PQ when ϑ_2 and ϑ_3 are taken as 30^0 and 60^0 respectively and for several values of inclination (ϑ_2) across the planar part QR when ϑ_1 and ϑ_3 are taken as 60^0 and 30^0 respectively. The rate of displacement is stated as follows:

$$\frac{\partial}{\partial t}[(v_3)_2 + (v_3)_3 + (v_3)_4]$$

From these figures, it is noticed that the rate of displacement increases continuously for both the cases with decrease in inclination. For $z_2 > 0$, rate of v_3 increases slowly and after attaining maximum value near $z_2 = 3\ km$ it decreases towards zero. But there is a very little impact of ϑ_2 on rate of change of v_3 which is shown from Fig. 2(b). It is obtained that the rate of displacement increases with decreasing value of ϑ_2 but this change of rate of v_3 is very little. After attaining highest value near $z_2 = 3$ km, it decreases towards zero. If the inclination across the planar part PQ is changed only and except this all others are fixed then the rate of displacement attains maximum value near about 1.3×10^{-3} meter/year. If the inclination across fault part QR only changed

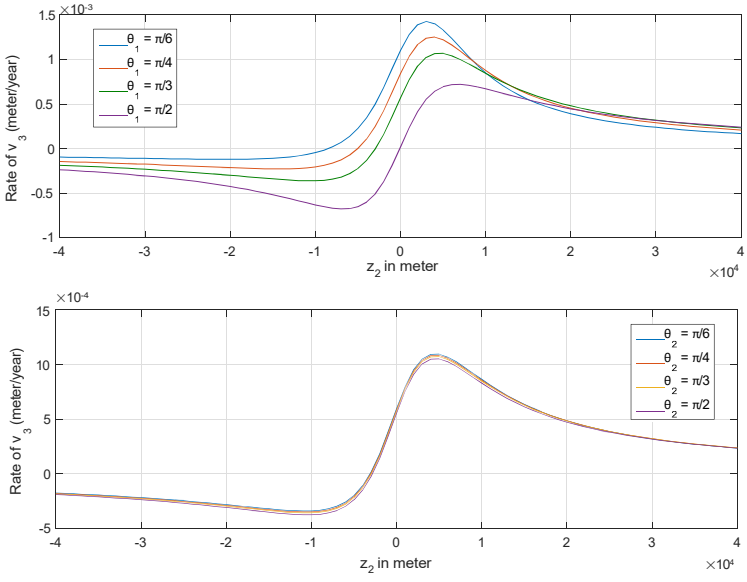

(a)

(b)

Fig. 2 *Variation of rate of displacement in z_3 direction against z_2 for several values of inclination (a) ϑ_1 across PQ and (b) ϑ_2 across QR*

then the maximum displacement across the fault is 1.1×10^{-3} meter/year (approximately). If we change the inclination (ϑ_3) across the planar fault part *RS* then there is no variation of the curves for different values of inclination which notified that if the parts of the fault spread out in downwards direction then there is a very little effect of the end parts of the faults being noticeable.

The influence of inclination ϑ_1 across the planar part *PQ* and ϑ_2 across the planar part *QR* on stress component for dip-slip movement (γ_{23}) is depicted through Figs. 3 (a) and (b) respectively. From Fig. 3 (a), it is observed that γ_{23} attains maximum value 7000 N/m^2 (approximately) near $z_2 = 0$. For $|z_2| \to \infty$, it decreases towards zero. For $z_2 > 0$, γ_{23} decreases with decreasing value of ϑ_1. After releasing all the stress (γ_{23}) near about $z_2 = 6$ km, it increases towards zero. From Fig. 3 (b), it is obtained that all the curves for different values of inclination (ϑ_2) across the planar fault part *QR* almost coincide. For $z_2 > 0$, γ_{23} releases all the stress near $z_2 = 3$ km and after that it increases towards zero. If we compare Fig. 3 (a) with (b), it is noticed that the stress releases very quickly across *PQ* part comparing to across *QR* part of the nonplanar fault.

5.2 Effect of velocity of the fault movement:

Figs. 4 (a), (b) and (c) delineate the impact of creep velocity on rate of displacement (v_3) in z_3 direction. These figures illustrated that the rate of displacement

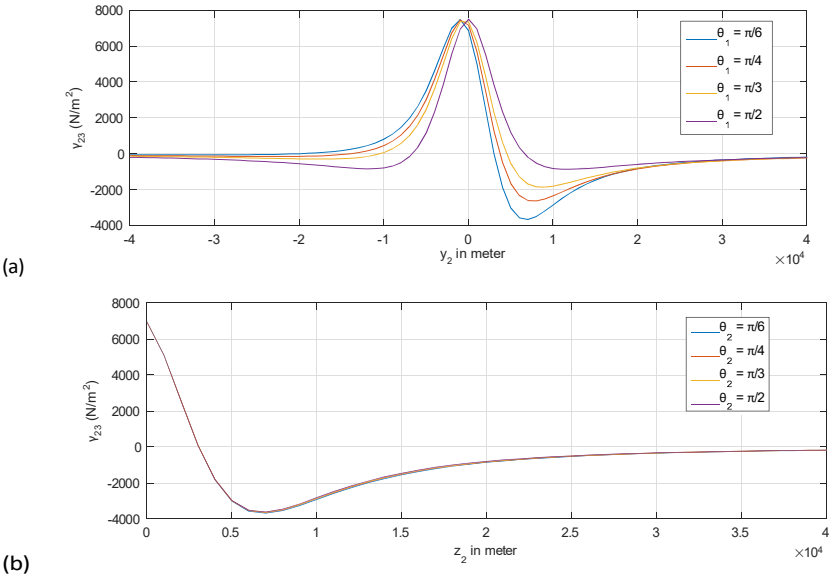

Fig. 3 *Variation of rate of stress γ_{23} against z_2 for several values of inclination (a) ϑ_1 across PQ and (b) ϑ_2 across QR*

increases continuously for all the cases with increasing value of creep velocity. For all the cases, rate of v_3 increases for $z_2 > 0$ and after attaining maximum value it is diminishing towards zero. Comparing Fig. 4 (a), (b) and (c), it is obtained that for different creep velocity across the fault part *PQ*, the change of rate of v_3 is more visible than across the fault part *QR*. Across the fault part *RS*, all the curves are coincide which shows that if the planar part *RS* of the nonplanar fault changes it velocity of movement then it does not effect on rate of displacement.

Figure 5 (a) and (b) represent the impact of velocity of the fault movement of first (PQ) and second planar parts (QR) of the nonplanar fault on rate of stress γ_{23} respectively. It is observed that γ_{23} increase with increasing value of velocity across *PQ*. For $y_2 \rightarrow \infty$ rate of γ_{23} increases and after attaining highest value it diminishing towards zero. But across the 2nd planar fault part *QR*, rate of γ_{23} coincide for different values of change of velocity. The reason behind the coincidence of the all the curve for different velocities may follow the fact that due to the downward position of the fault part QR and since the fault movement is dip-slip type then all the planar fault parts of the nonplanar fault are situated in downward direction.

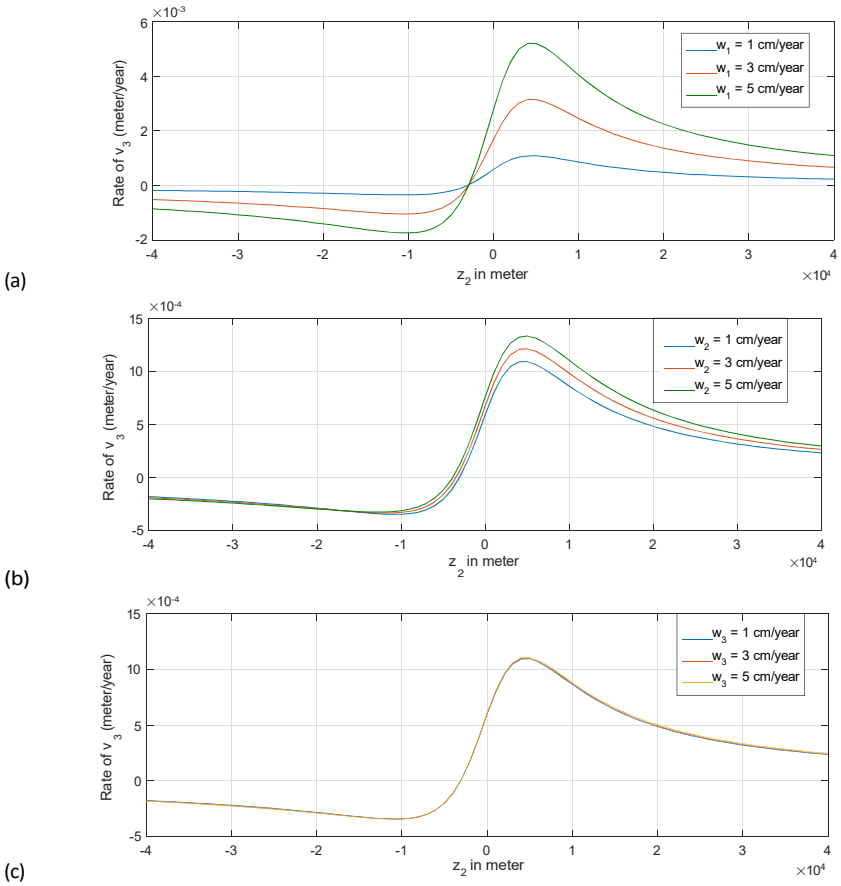

Fig. 4 *Variation of rate of displacement in z_3 direction against z_2 for several values of creep velocity (a) w_1 across PQ, (b) w_2 across QR and (c) w_3 across RS*

5.3 Effect of depth of the fault from the free surface:

Figure 6 (a) and (b) illustrate the impact of depth of the fault parts PQ from the free surface and depth of the fault part QR from PQ on rate of displacement. It has been examined that the rate of displacement increases with diminishing value of the depth r_1 across PQ. For $y_2 > 0$, it increases and attains maximum value. After attaining maximum value, rate of v_3 decreases towards zero. Also rate of displacement increases with diminishing value of depth r_2 across QR from the fault part PQ. But there is a very small difference. The cause behind this behavior may follow the fact that as the 2nd planar fault part QR of the nonplanar fault lie in downward position due to dip-slip movement of the fault.

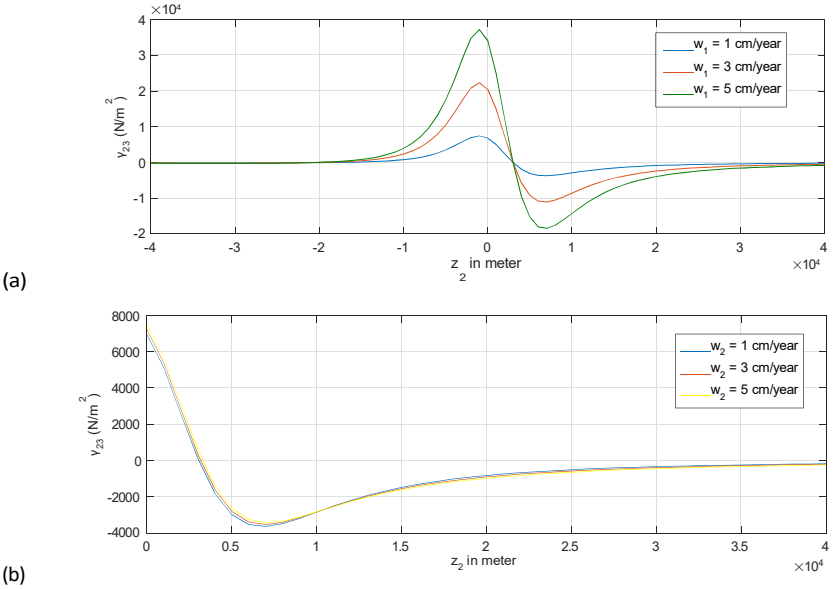

Fig. 5 *Variation of rate of stress γ_{23} against z_2 for several values of creep velocity (a) w_1 across the first planar parts PQ and (b) w_2 across the 2nd planar part QR*

The effect of depth across the first planar fault part PQ of the nonplanar fault on rate of γ_{23} has been described in Fig. 7. It is reported from this figure that the increases of depth from the free surface causes decrease in the rate of γ_{23}. It may be due to the reason that as if we go in the downward from the earth's surface then the effect of ground movement with be diminishing. The rate of γ_{23} accumulates maximum value near $y_2 = 0$ and after that it releasing all the stresses and going towards zero.

5.4 Effect of time of occurrence of the fault movement:

Fig. 8 described the impact of time of occurrence of fault movement on rate of change of displacement. It shows that the rate of displacement due to the nonplanar fault movement is increases with time. The variation of strain component e_{22} with time has been illustrated in Fig. 9. This figure shows that when the fault movement occur then maximum strain accumulated and after that all the accumulated strain releases with time. The releasing amount of energy effect on the ground which can be a cause of next major earthquake.

5.5 Effect of fractional order (α):

Rate of change of stress component (γ_{23}) for dip-slip movement with time (t_1 in year) for different values of the order of fractional derivative α has been

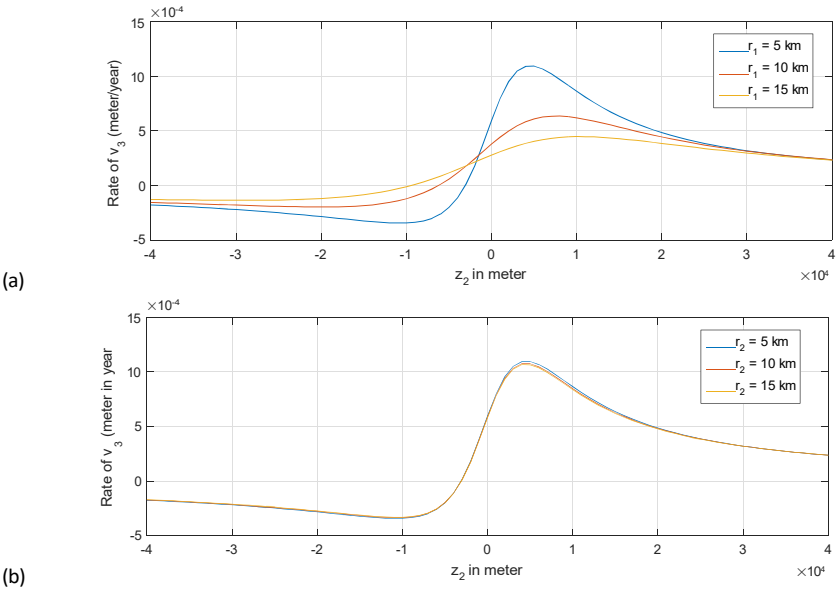

Fig. 6 *Variance of rate of displacement for different values of (a) depth r_1 from the free surface across the part PQ and (b) depth r_2 across the part QR from PQ.*

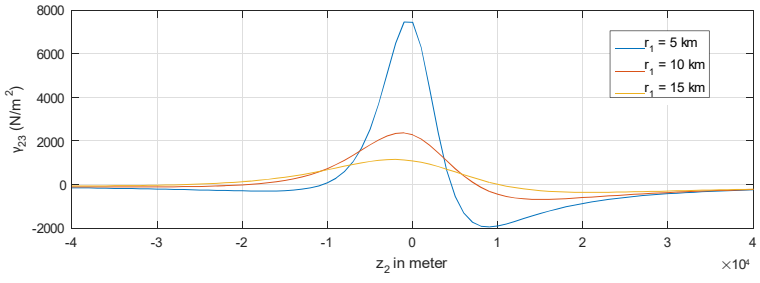

Fig. 7 *Variance of rate of γ_{23} for different values of depth r_1 from the free surface across the part PQ*

plotted in Fig. 10. For $y_2 > 0$, γ_{23} increases with time and also it increases with expanding value of fractional order derivative (α). It indicates that this fractional order has a significant impact on the rate of change of γ_{23}.

6 Comparison

In this present model, the fault is taken as nonplanar fault which is interconnected by three planar parts. Comparing this study with Mahato et. al (2022 [17]) where the effect of ground deformation due to planar fault in fractional

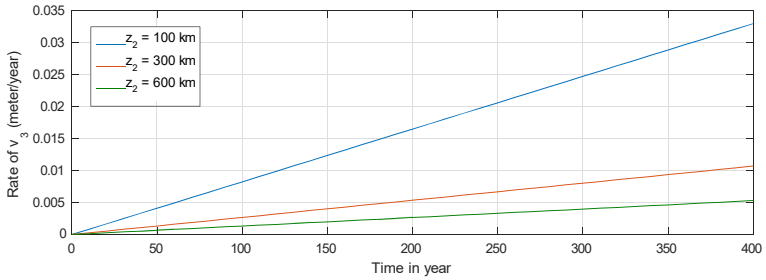

Fig. 8 *Variation of rate of change displacement with time (t) of occurrence of fault movement for different values of z_2*

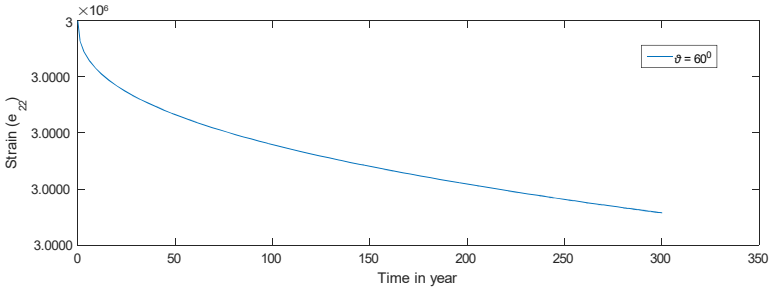

Fig. 9 *Variation of strain (e_{22}) with time (t) of occurrence of fault movement*

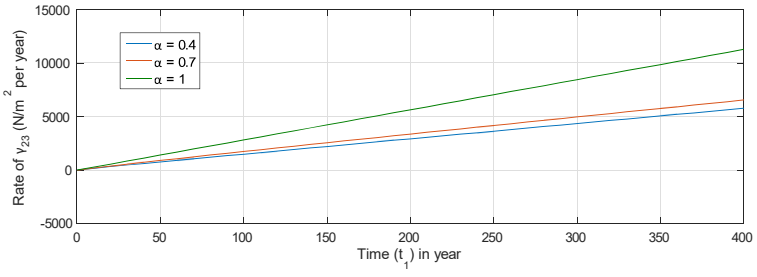

(a)

Fig. 10 *Change of rate of stress (γ_{23}) against z_2 due to fault creep for different order of fractional derivative α*

calculus method has been observed, it is found that the displacement (v_3) due to movement across nonplanar fault is more than planar fault. It is also obtained that a huge amount of stress accumulated if the fault model is non planar which indicates that if the fault will be nonplanar then the effect on the ground is more than the planar fault. From this comparative study, it is concluded that if in a certain place a nonplanar fault movement occur then

the huge amount of accumulated stress in aseismic period will be released in seismic period which effects more on the neighbourhood of the fault plane.

7 Conclusion

The present work advances the theoretical knowledge regarding the effect of non-planar fault geometries on earthquake mechanics. We have introduced a method to observed a non-planar earthquake fault geometries using a few parameters. The non-planar fault surfaces are connected with three planar parts. By expanding the relation of displacement, stress and stain components with y_2 axis across different planar parts of the non-planar fault from a planar fault, this study allows for the interpretation of complex fault geometry and its impact on displacement and stress-stain components. The following outcomes of the present study are encapsulated below:

(i) The displacement due to fault movement in dip direction discourage with increasing value of inclinations. If the fault is vertical then the displacement due to the fault movement is less than the fault with inclined angle.
(ii) The impact of inclination on stress component (γ_{23}) has an amplifying effect. If the inclination across the fault increases then the accumulation of stress also increases. So, if the fault is vertical with the free surface then a huge amount of stress will be accumulated which may help to occur a indestructible earthquake.
(iii) The velocity of the fault movement has an decaying effect on displacement and stress components. If the velocity of the fault movement increases then the fault displace more with a high rate of accumulation stress.
(iv) The displacement and accumulated stress are decreases with increasing values of depth.
(v) The accumulated stress releases with time and this releases amount of stress caused displacement due to fault movement.
(vi) The fractional order derivative (α) has been considered in the range $0 < \alpha < 1$. The effect on displacement and stress-strain accumulation of a fractional model is more prominent than the integer model.

This model can be extended for various geological scenarios, including surface breaking/locked faults, facilitating the analysis of stress and strain distribution. Also the medium can be chosen as a viscoelastic half-space of Burger's Rheology or a layered media, overlying a viscoelastic half-space. The mathematical models of nonplanar faults emerge as a promising avenue for future research in this field.

Conflict of Interest

No potential conflict of interest was reported by the authors.

References

1. Aki, K., Richard, P.G.: Quentitative Seismology, 2ed edn. University Science Books, Sausalito (2002)
2. Bouchez, J.-L., Nicolas, A.: Principles of Rock Deformation and Tectonics.OxfordUniversity Press, Oxford (2021). https://doi.org/10.1093/oso/9780192843876.001.0001
3. Cathles, L.M.: The Viscoelasticity of the Earth's Mantle. Princeton University Press, Princeton (1975)
4. Debnath, S.K., Sen, S.: Movement across a long strike-slip fault and stress accumulation in the lithosphereasthenosphere system with layered crust model. Int. J. Sci. Innov. Math. Res. 2(9), 770–781 (2014)
5. Debnath, P., Sen, S.: A vertical creeping strike slip fault in a viscoelastic half space under the action of tectonic forces varying with time. IOSR J. Math. (2015). https://doi.org/10.6084/M9.FIGSHARE. 1410995.V1
6. Caputo, M.,Linear models of dissipation whose Q is almot frequency independent-II, Geophysical Journal International, 13, 529-539 (1967).
7. Chift, P., Lin, J., Barcktiausen, U.: Evidence of low flexural rigidity and low viscosity lower continental crust during continental break-up in the South China Sea. Mar. Pet. Geol. 19, 951–970 (2002)
8. Chinnery, M.A.: The deformation of the ground around surface faults. Bull. Seis. Soc. Am. 51, 355–372 (1961).
9. Chinnery, M.A.: The stress changes that accompany strike-slip faulting. Bull. Seis. Soc. Am. 53, 921–932 (1963)
10. Chinnery, M.A.: The strength of the Earth's crust under horizontal shear stress. J. Geophys. Res. 69, 2085– 2089 (1964)
11. Chinnery,M.A., Jovanovich, D.: Effect of Earth layering on earthquake displacement fields. Bull. Seis. Soc. Am. 62, 1969–1982 (1972)
12. Debnath, S.K., Sen, S.: Movement across a long strike-slip fault and stress accumulation in the lithosphereasthenosphere system with layered crust model. Int. J. Sci. Innov. Math. Res. 2(9), 770–781 (2014).
13. Fowler, A.C.: On the thermal state of earth's mantle. J. Geophys. 53, 42–51 (1983)
14. Karato, S.: Rheology of the earth's mantle. A historical review. Gondwana Res. 18(1) (2020)
15. Kundu, P., Sarkar (Mondal), S., Rashidi, A., Dutykh, D.: Comparison of ground deformation due to movement of a fault for different types of crack surface. GEM Int. J. Geomath. (2021). https://doi.org/10. 1007/s13137-021-00171-5
16. Li, Z., Wang, T.: Coseismic and Early Postseismic Slip of the 2021 Mw 7.2Nippes, Haiti, Earthquake: Transpressional Rupture of aNonplanar Dipping Fault System, Seismological Research Letters (2023) 94 (6): 2595–2608. https://doi.org/10.1785/0220230160
17. Mahato, P., Mondal, D. and Sarkar (Mondal), S.: Determination of effect of the movement of an infinite fault in viscoelastic half space of standard linear solid using fractional calculus, Phys. Scr. 97 (2022). https://doi.org/10.1088/1402-4896/ac9caa
18. Marshall, S.T., Cooke, M.L., Owen, S.E.: Effects of nonplanar fault topology. Bull. Seismol. Soc. Am. (2008). https://doi.org/10.1785/0120070159

19. Maruyama, T.: Static elastic dislocations in an infinite and semi-infinite medium. Bull. Earthq. Res. Inst. Tokyo Univ. 42, 289–368 (1964)

20. Maruyama, T.: On two dimensional dislocation in an infinite and semi-infinite medium. Bull. Earthq. Res. Inst. Tokyo Univ. 44(3), 811–871 (1966)

21. Mondal, D., Kundu, P., Sarkar, S.: Accumulation of stress and strain due to an infinite strike-slip fault in an elastic layer overlying a viscoelastic half space of standard linear solid (SLS). Pure Appl. Geophys. (2020). https://doi.org/10.1007/s00024-020-02536-7

22. Mondal, S.C., Sen, S., Debsarma, S.: A mathematical model for analyzing the ground deformation due to a creeping movement across a strike slip fault. GEM Int. J. Geomath. (2019). https://doi.org/10.1007/ s13137-019-0129-3

23. Mondal, S.C. and Debsarma, S: Numericalmodelling of a nonplanar strike slip fault and associated stress distribution in lithosphere asthenosphere system, GEM - International Journal on Geomathematics (2023) Vol -14(15) https://doi.org/10.1007/s13137-023-00222-

24. Mukhopadhyay, A., Sen, S., Pal, B.P.: On stress accumulating in a viscoelastic lithosphere containing a continuously slipping fault. Bull. Soc. Earthq. Tech. 17(1), 1–10 (1980a)

25. Rybicki, K.: The elastic residual field of a very long strike-slip fault in the presence of a discontinuity. Bull. Seis. Soc. Am. 61, 79–92 (1971).

26. Scott T. Marshall, Michele L. Cooke, and Susan E. Owen: Effects of Nonplanar Fault Topology and Mechanical Interaction on Fault-Slip Distributions in the Ventura Basin, California, Bulletin of the Seismological Society of America, 98, 1113–1127 (2008), doi: 10.1785/0120070159

27. Segall, P.: Earthquake and Volcano Deformation. Princeton University Press, Princeton (2010)

28. Sen, S., Karmakar, A., Mondal, B.: A nonplanar surface breaking strike slip fault in a viscoelastic half space model of the lithosphere. IOSR J. Math. 2(5), 32–46 (2012)

29. Sen, S., Karmakar, A.: The nature of stress pattern due to a sudden movement across a nonplanar buried strike-slip fault in a layered medium. Eur. J. Math. Sci. (2013). https://ejmathsci.org/index.php/ ejmathsci/article/view/144

30. Singleton, D.M., Maloney, J.M., Brothers, D.S., Klotsko, S., Driscoll, N.W., Rockwell, T.K.: Recency of faulting and subsurface architecture of the San Diego bay pull-apart basin, California, USA. Front. Earth Sci. 9, 641346 (2021). https://doi.org/10.3389/feart.2021.641346

31. Steketee, J.A.: On Voltera's dislocation in a semi-infinite elastic medium. Can. J. Phys. (1958a). https://doi. org/10.1139/p58-024

32. Steketee, J.A.: Some geophysical applications of the theory of dislocations. Can. J. Phys. (1958b). https:// doi.org/10.1139/p58-123